How to Cite:
Gopagoni, D. R., & Lakshmi, P. V. (2022). Deep learning enthused hybrid framework for early diagnosis of mild cognitive disorder caused by Alzheimer's disease. *International Journal of Health Sciences*, *6*(S2), 9516–9533. https://doi.org/10.53730/ijhs.v6nS2.7502

Deep learning enthused hybrid framework for early diagnosis of mild cognitive disorder caused by Alzheimer's disease

Deepa Rani Gopagoni
Department of Computer Science and Engineering, GIT GITAM (Deemed to be University) Vishakhapatnam, Andhra Pradesh, India

P V Lakshmi
Department of Computer Science and Engineering, GIT GITAM (Deemed to be University) Vishakhapatnam, Andhra Pradesh, India

***Abstract*---**Put Memory cells in the brain are permanently damaged in Alzheimer's disease, making it a common cause of dementia. It is possible that early diagnosis of this condition may aid medical professionals in the treatment of patients and the prevention of disease progression. Anatomical changes in the brain's diseased context may be assessed by MRI (magnetic resonance imaging), regardless of other neuroimaging-based diagnostic procedures. MRI diagnosis has shown generally sufficient results in terms of classifying the MRI picture from normal to Alzheimer's disease, according to existing research papers on the subject. However, in many clinical circumstances, MRI results are indifferent between the normal controls and the MCD (Moderate Cognitive Decline/Impairment) phase of the study time frame. For this challenge, a deep learning inspired optimization model is presented in the study that helps in the correct classification of MRIs of normal and MCD. Experiments have shown that the suggested model outperforms a number of current methods for picture segmentation.

***Keywords*---**Alzheimer's disease, MCD, image analytics, deep learning, optimization.

Introduction

A medical technology, generally acknowledged in the identification of neuropathological illnesses such as Parkinson's disease, Huntington's disease, and Alzheimer's disease (AZD), neuroimaging is frequently used. According to reports, AZD is responsible for more than 70% of all instances of dementia in the general population. Currently, it is considered to be a rapidly expanding

neurodegenerative phenotype that affects around 50.4 million individuals across the globe. The majority of the symptoms shown by the afflicted individuals involve a decline in cognitive skills, which has a substantial impact on their daily lives and their normal environment, according to the researchers. A few pieces of evidence-based study suggested that the cost of patients experiencing AZD in conjunction with dementia would be around 2.5 trillion dollars by 2030. As a result, the design and development of early interventional strategies that assist an individual and a medical professional in the context of diagnosing, preventing, and restricting the progression of dementia-related symptoms are considered to be an important facet of research in the field of medical image.

In spite of the fact that the brain has traditionally been considered a soft tissue organ, magnetic resonance imaging (MRI) is now considered a trustworthy and effective approach for detecting key pathologically relevant anatomic abnormalities of the brain. MRI Magnetic resonance imaging (MRI) has been the gold standard for the diagnosis of MCD and AZD in recent years because of its astringent properties. Referring to figure 1, it can be seen that clinical analysis and diagnostic outcomes have typically been good for the AZD using the MRI method, with images being classified as either normal or indicative of an illness such as an AZD. A considerable number of clinical evaluations show that magnetic resonance imaging (MRI) is insensitive throughout the time between normal controls and moderate cognitive decline/impairment (MCD). An analysis of data shows that the MCD's picture characteristics seem to match the AZD's in general, which means that normal image classifiers will have difficulty categorising different age groups during the two stages of AZD. Artificial intelligence and deep learning algorithms are primarily used in this study to evaluate and appraise the relevance of overcoming the restriction implied by the pathological differentiation involved in each phase of AZD.

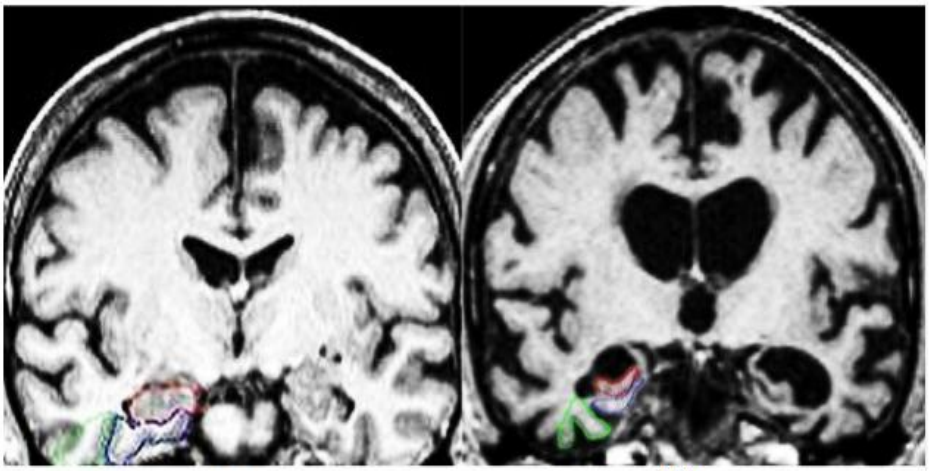

Figure 1: (a) Normal MRI (b) Alzheimer's MRI

There have been recent studies showing that various optimization techniques, including Particle Swarm Optimization (PSO), Ant Colony Optimization (ACO), the

Cukoo Search algorithm (CS), Grey wolf optimization (GWO), etc., were applied during the process of segmenting images, where it was shown that their performance was greatly improved when selecting the appropriate threshold value while deriving global solutions. Following these studies, we hope to contribute an image segmentation framework for multimodal image segmentation that incorporates the optimization of global optimal threshold values and deep learning architecture for the accurate classification of normal control images from AZD images by using the modified U-net based deep learning architecture.

Preliminaries

Multi-Level Thresholding using Optimization Algorithms

When using multi-level thresholding in image segmentation, the primary goal is to find the ideal threshold value for acquiring desirable features from the desired features in an MRI image, depending on the variation of the selected optimization function. Researchers have been obliged to use multi-level thresholding because of the limits of single-level thresholding, which may be considered an optimization approach. An important part of tackling complicated issues with limited resources and time is the use of these optimization methods. Kapur's entropy-based optimization and Otsu's optimization are two well-known and basic optimization approaches that are often used to segment biological pictures without previous information. Genetic algorithms (GA), Particle Swarm Optimization (PSO), Cuckoo Search (CS), Bat Algorithm (BA), and Firefly Algorithm (FA) [1,2] are among methods that may be used.

Bio-inspired optimization algorithms have been shown to be flexible, simple, and more effective at finding the global optimal solution than other strategies used to identify the local one. In order to extract the desired feature, grey level thresholding is considered an adaptive feature extraction process that eliminates the object's backdrop. For precise performance, it's vital to find the optimal optimization function, which makes determining the threshold values difficult. There have been several studies on different objective functions, such as Kapur entropy [3], Otsu entropy [4], Cross entropy [5] and Fuzzy entropy [6]. Numerous works use Genetic Algorithm (GA) hybrids to solve multilevel thresholding problems [7]. The evolutionary algorithm created by Zhang et al. [8] uses quantum computing and incorporates multiple thresholds, an adaptive adjustment technique, and an adaptive learning mechanism. That it outperforms other optimization techniques such as PSO (and CS) is shown by simulation results Using the goal function of Kapur and otsu entropy, the authors in [9] created a hybrid multimodel approach to solve multilevel thresholding. Experiments show that this hybridization outperforms other current methods in comparison. Segment the AZD using GAN's [10] and the conditional characteristic. In comparison to more traditional methods, this one also utilises a two-stage network. There is nevertheless a generator in the first network and a discriminator in the second network. An input colour fundus picture and an output binary mask are used to train the generator network, which then maps the anticipated and ground truth information using a loss function. [11]. The model is inspired by ResNet-50, which is based on the modified U-Net and Depth First Select graph approach. The midpoint of AZD and its probability map is selected

by this network. The D-FS algorithm then selects the brightest and most frequent location on the probability map as the most probable AZD. An object detector for AZD segmentation using the Faster-RCNN [12] has been suggested. First, this object detector uses its bounding box discovery to estimate the appearance of AZD before finding another bounding box that can also yield an ellipse-like bounding box. CNNs, like those used in [13], attempt to visualise an AZD's boundary box and its associated probabilities and confidence ratings.

When PNet is used to create an initial segmentation map with low resolution and Fine-net is used to upscale the received map to higher resolution, an improved method of segmentation is provided [14]. Segmenting the AZD based on RoI has been explored by the author. The FCN and U-Net architecture are usedin this approach. The model [15] is a comparison. Faster-RCNN is another method [16] for detecting the bounding boxes of AZD. By using this approach, the simple characteristics that should be learnt during the training phase are separated from the more difficult ones that may be taught during the testing stage. If the projected outcome is correct, then we may classify the area as AZD or Non-OD. A variety of optimization methods, including CNNs, have been used to improve the accuracy of feature selection and classification in a variety of medical pictures. It is hoped that through this research, which is motivated by cutting edge mechanisms, a multimodal framework for deep learning-inspired feature extraction from MRI images will be developed, which will allow researchers to distinguish and accurately identify the differences between normal control MRI and MCD MRI.

Dataset Collection

The Alzheimer's disease Neuroimaging Initiative (ADNI) dataset was used in many state-of-the-art research projects, including 156 AZD cases, 189 MCD cases, and 130 suspected cases, totalling 475 cases. The Open Access Series of Imaging Studies (OASIS)[17]dataset was used in this work, which includes the open source collection of MRI scans from the different phases of AZD. Also included is a cross-sectional dataset comprising roughly 420 participants, aged between 18 and 98 years old. Also included is a longitudinal data collection that contains data from 60-98-year-olds who are either demented or not. According to medical specialists, AZD's development should be monitored for around 18 months at a minimum.

Many research use the ADNI dataset to categorise and explain the transformative shift in AZD as mentioned. One of the primary goals of studying the ADNI dataset is to see whether it can be used to track MCD and the early phases of AZD development utilising the many clinical biomarkers such as PET, MRI, neuropsychological assessments, and others. T1-weighted, organised 1.5T MRI scans are used to build the ADNI dataset at the beginning of the study. In this research, the data gathered from the OASIS dataset, which contains MRI scans of the brain's interior regions, such as the white and grey matter as well as the corpus callosum and the hippocampus, is the focus. The primary goal of this research is to distinguish between the MRI scans of participants in the early stages of the AZD. As a result, the planned study would use 2D T2-weighted MRI brain images to gauge the framework's efficacy. These slices of the brain MRI are

derived from the OASIS database, where 1.5T scans are used to generate these pictures. The resulting pictures feature diameters of 1mm spacing and a thickness of 5mm with a 256*256 resolution. To conduct this research, collected photos from 435 individuals ranging in age from a variety of healthy individuals and AZD sufferers. Accordingly, this research only examines coronal slices of brain to segment Hippocampus and to segment Corpus Callosum since it is primarily concerned with AZD early identification.

Two-Dimensional Maximum Entropy

Images are assessed by looking at the image's 2D-maximum entropy, which in most situations yields the 2D histogram.

$$H_{ij} = P_{ij} / N*N \quad \ldots \qquad (1)$$

If the average local pixel value is 'j,' then Pij represents the total number of pixels with a grey value equal to 'i. N*N is the total number of pixels in the picture, which is indicated by the N*N. Here are some examples of how the two-dimensional histogram plane could be described:

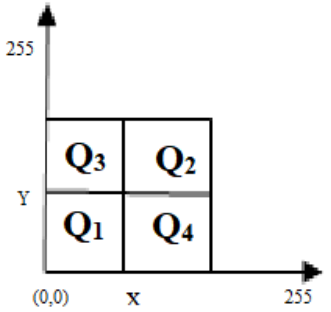

Figure 2: 2D histogram Plane

The areas indicated by Q3 and Q4 in the above histogram represent the edge and noise of the MRI image, respectively, whereas the areas denoted by Q1 and Q2 represent the background and foreground of the item in the MRI picture, respectively. Furthermore, as shown in the histogram (X, Y) above, X signifies the threshold value connected to the intensity of the pixels, and Y shows the local average of the pixels, where X is the threshold value related to the intensity of the pixels. It is explained by the maximum entropy rule that the maximum information about a picture should be retrieved from Q1 and Q2 when a specified threshold value is reached.

Proposed Framework

A framework for multi-objective optimization was spawned by the deep learning model provided in Figure 3. There are five steps to this process. The first is to obtain brain MRI scans through OASIS database, the second is to apply the 2D-Fuzzy Tsallis maximum entropy mechanism to preprocess the data before looking for a global optimum threshold value in areas of interest like the Corpus callosum

and the Hippocampus. The third step is to apply the invasive weed optimization mechanism. In order to train and test the MRIs, a U-Net based CNN architecture is used, and eventually, the ground truth information is created.

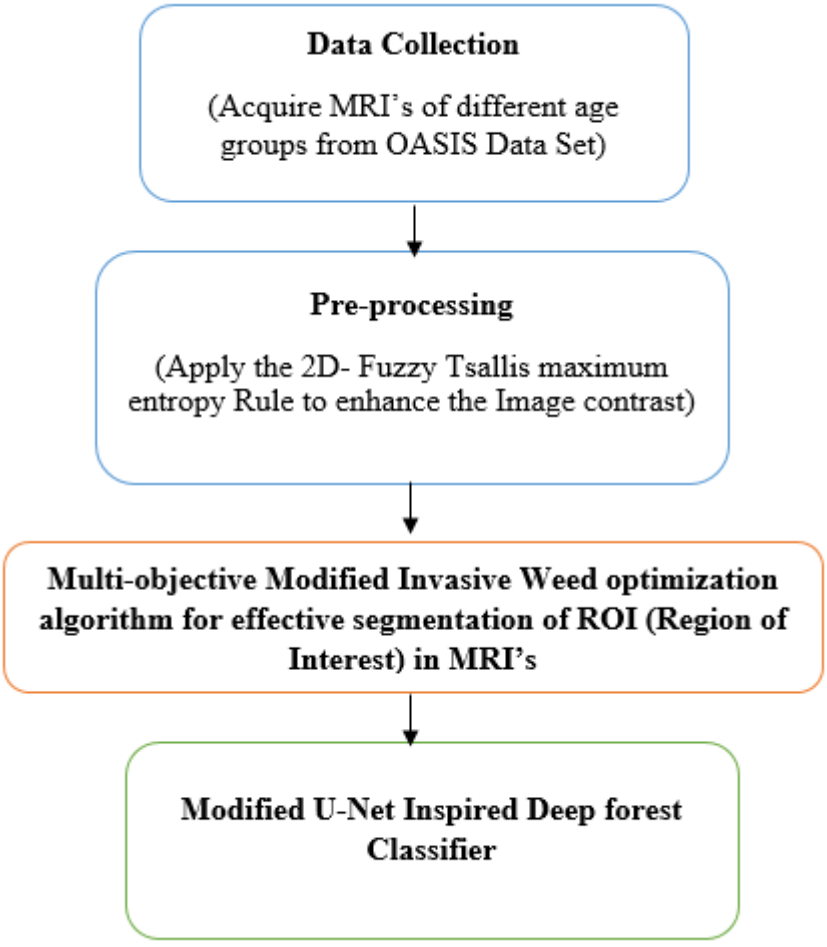

Figure 3: Proposed Framework

Pre-Processing

In the OASIS database, MRI's of different people from various hospitals are included, and since all of the photographs are taken at the same intensity, the background area and object quality are both degraded. Additionally, it has been determined that segmenting the interior parts of the brain would be a difficult process owing to the same intensity of the pictures. The suggested study is meant to categorize MRI's that contain the corpus callosum and the Hippocampus, and as a result, it is necessary to increase the contrast of the images in order to identify the area in which they are shown. For the purpose of preprocessing, fuzzy Tsallis entropy is used in conjunction with skull stripping to get the desired

result. Initially, during the process of incorporating fuzzy set theory into image segmentation, the digital picture created is treated as a fuzzy set, with the background and the object having a restricted membership function, as shown in the table below:

$$\vartheta_a\big(V(P,avg)\big) + \vartheta_b\big(V(P,avg)\big) = 1 \text{ ---- (2)}$$

In which ϑ_a, $\vartheta_b$is used to represent a membership function for a certain background and object, such that (P, avg) represents the decomposition of the vectors at grey level of pixel P of an average of neighbors. During the thresholding procedure if ϑ_a>$\vartheta_b$the grey layer of the picture is subsequently propagated as an object, and the reverse is also true.

$$\vartheta_a\big(V(P,avg)\big) = \begin{cases} 1,\ D(V) \le D(V_a) \\ \frac{D(V-V_a)}{D(V_a-V_c)}, D(V_a < D(V) < D(V_c) \\ 0,\ D(V) \ge D\ (V_c) \end{cases} \quad \text{---- (3)}$$

Avg (P,avg) and vector(0,0) are shown in equation 3 as the composition of the grey levels of the neighbouring average and pixel 'p', and D(V) is the Euclidian distance in between them.

$$D(V) = \sqrt{P^2 + avg^2} \text{---- (4)}$$

Following a computation of the fuzzy set's range, a suitable threshold may be found.

$$K^{opt} = \frac{(V_a^{opt} + V_b^{opt})}{2} \text{---- (5)}$$

Image Segmentation using Modified IWO(Invasive Weed Optimization)

One of nature's most sophisticated approaches, the Invasive Weed Optimization Algorithm (IWO), is a powerful tool. An agriculture miracle known as the colonization of obnoxious weeds is used in this estimate. Plants that thrive in unsuitable locations are known as weeds. They have a lot of muscle and are known for their adaptability.

Weeds have the unique ability to repopulate an area with an overwhelming majority of their original population. The IWO computation is broken down into the basic steps that include the next epoch generation, Dispersion in space disposal should be taken seriously in this case. Only a small number of distinct foci are generated in the statement phase. These points of interest are scattered across the hunting area. The supplied point's component is compared to the thresholding level n. It is assumed that each point has homogeneous dispersion between the upper limit U and the smallest cutoff L. The population size m refers to the number of plants that were harvested at a certain location.

Algorithm: Modified IWO

Procedure IWO-M

1. *Input: Set of parameters used for parameter tuning for IWO to determine optimal threshold*
2. *Output: Optimal threshold*
3. *Generate invasive weed solutions randomly using fuzzy tsallis entropy indicated in 3.4.1*
4. *While* $Search_{num}$*< population do*
5. *for every weed do*
6. *compute the number of seeds;*
7. $weed_n = \frac{K-K_{max}}{K_{min}-K_{max}}(l_{max} - l_{min})$;
8. *Update* ϑ
9. $\vartheta_{current} = \frac{Iteration_{max}-Iteration}{iterationmax}$
10. *for every seed compute fitness value*
11. *If seed < threshold then*
12. *Select (bst_seed)*
13. *Endif*
14. *End for*
15. *End for*

Modified U-Net inspired Deep Forest classifier

Pixel-wise image segmentation challenges have demonstrated superior results for CNNs than conventional techniques. The purpose of CNN is to decipher an image's feature mapping by applying a variety of feature mapping gradations. While for the segmentation job, transforming a feature map to a vector and then reconstructing an image from this vector are both critical tasks. These types of issues were addressed by the U-Net design [18]. Using this approach, U-Net was able to take first place in the 2015 ISBI challenge[19]. As shown in Figure 4, the architecture of the U-Net flavour is suggested in this article, and it can greatly decrease distortion by showing the structural integrity of an image, as demonstrated in Figure 4. There are three stages to this architecture: contraction, bottleneck, and growth.

Two 3X3 convolution layers follow by a 2X2 max-pooling with a stride of two make up the five contraction blocks that make up the contraction section. The kernel begins with a size of 16 and grows by two blocks at a time until it reaches a maximum of 256 to allow the architecture to efficiently learn increasingly complex structures. A 2 X 2 up convolution layer mediates the contraction and expansion layers in the bottleneck portion, which employs 3 X 3 CNN layers. The core of the building's design is its extension portion.

There are exactly as many blocks as there were in the contraction layer, ensuring that all of the characteristics learnt during the contracting process may be utilized to recreate an image when it is reconstructed. There are three 3 X 3 CNN layers followed by two 2 X 2 upsampling layers in each of the blocks in the

expansion layer of the neural network. The input is mixed with feature maps from the relevant contraction layer, however, each time it is used. It is possible to ensure that each layer in the expansion section has sufficient information by using this strategy, which eliminates the issue of gradient vanishing. When executing convolutions that create outputs that are the same size as the input, the padding mode "same" is employed.

Two measures, Intersection over Union (IoU) and Accuracy, were employed to assess the model's effectiveness [20]. When it comes to semantic segmentation, the IoU measure is also known as the Jaccard Index, which is one of the most often employed metrics. In its most basic form, IoU operates by dividing the total number of pixels present across both the ground truth and anticipated images by the total number of pixels present across both. Rather of calculating the IoU score for each individual class, the mean IoU score is calculated by taking the average of all of the courses. For semantic segmentation, IoU and Accuracy are the ideal metrics to use when evaluating a model's accuracy and effectiveness. Here's how you can tell whether something is true:

$$Accuracy = \frac{TP+TN}{TP+FP+TN+FN} \text{----} \quad (6)$$

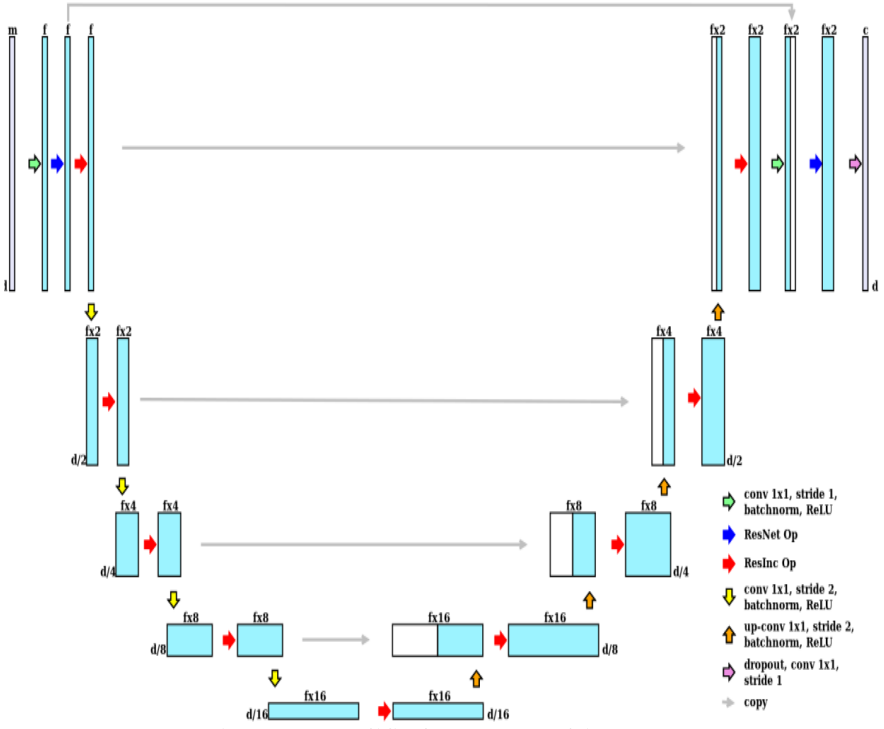

Figure 4 Modified U-Net Architecture

Modified Deep Forest Classifier (DFC)

The Deep Forest [21] is an ensemble-based decision tree approach that emphasizes building deep models using modules that arenon-differentiable.It is

built around thre eprimary principles that are considered the reasons behind the rich accomplishments of deep models. The reasons are as follows:

- Layer by Layer processing: It is considered one of the significant factors since, no matter how complex the flat model becomes, the features of layer by layer processing cannot beachieved.
- In-model feature transformation: Basic machine learning models work on the original set of features. However, new features are generated during the learning process of a deep model.
- Appropriatemodelcomplexity:Largedatasetsneedcomplexmodels,basicmachine learningmodelsarelimitedintermsofcomplexity.
  However,it is not the case with deep models.

The overall structural working of the deep forest is separated into two broad parts Cascade Forest Structure & Multi-Grained Scanning. Cascade forest structure ensures layer-by-layer processing, while Multi-grained scanning allows the model to achieve sufficient complexity.

Cascade ForestStructure

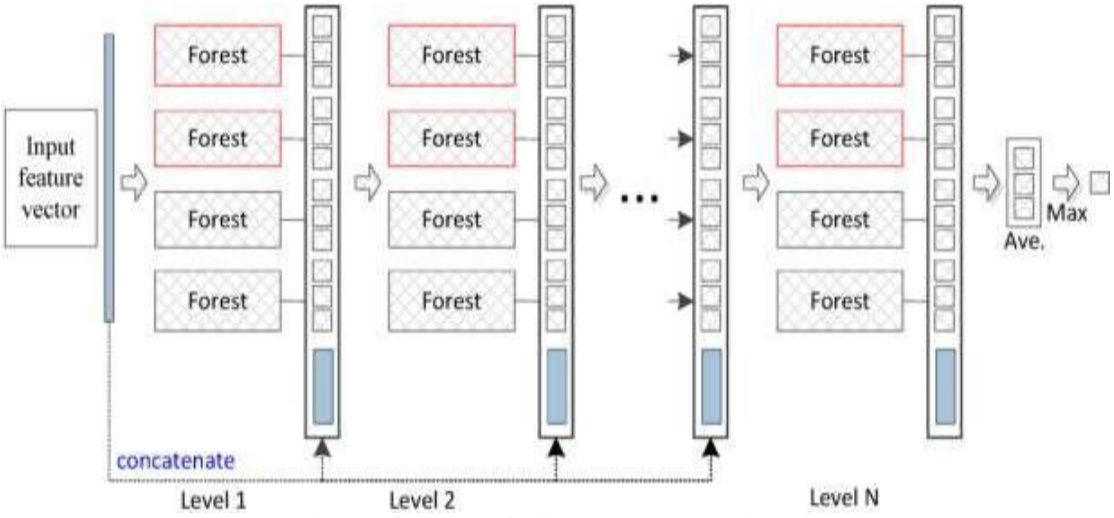

Figure.5. Cascade forest construction

Acascadestructureisemployedtorepresentthelayer-by-layer processing of raw features. Each layer in the cascade takes input (processed information) from the previous layer and feeds it into the next layer. A layer in the structure can be defined as an ensemble of decision tree forests. It is ensured that diversity is maintained while creating ensembles by including different kinds offorests. The working in cascading stage proceeds as follows, for a given case, an approximate class distribution will be generated by each forest. This is done by considering the training example sand fraction of different classes at the terminalorleafnodewheretheparticularinstancefalls, then averaging all the trees in the same forest. This has also been depicted in Figure. 5.

Theapproximatedclassdistributionsoobtainedformsavectorofclasseswiththehelpofk -fold cross-validation.

Thevectoristhenconcatenatedwiththeoriginalsetoffeatures.Theresultisthenforwarde d to the next cascading layer. K-fold cross-validation helps in reducing the risk of overfitting. The number of levels is determined automatically based on the performance of the validationset [22,23]. A striking difference in deep forest and other deep models is the ability to adaptively change the model complexity by terminating the amount of training data when tolerable. This provides a considerable advantage when working with datasets of varying sizes.

Multi-GrainedScanning

The cascading forest procedure is enriched with the procedure of multi-grained scanning. The inspiration behind the multi-grained scanning procedure was that deep models are generally well suited and good at handling feature relationships. The whole process is depictedinFigure3.The sliding windows and feature vectors scan raw features are produced. The feature vectors are either negative or positive based on the extraction from the training sample;they are thenusedtoproduceclassvectors[24].Acompletelyrandomforestistrained using the instances extracted from windows having the same size. The concatenation of generated class vectors obtains transformed features. The actual label of the training sample is used to assign the instances that are extracted from the windows. Though these assignments can be incorrect, they can be attributed to the flipping output method. Also,feature sampling can be performedif transformed feature vectorsaretoolong. Thesliding windows size is varied to obtain grained features vectors that aredifferent.

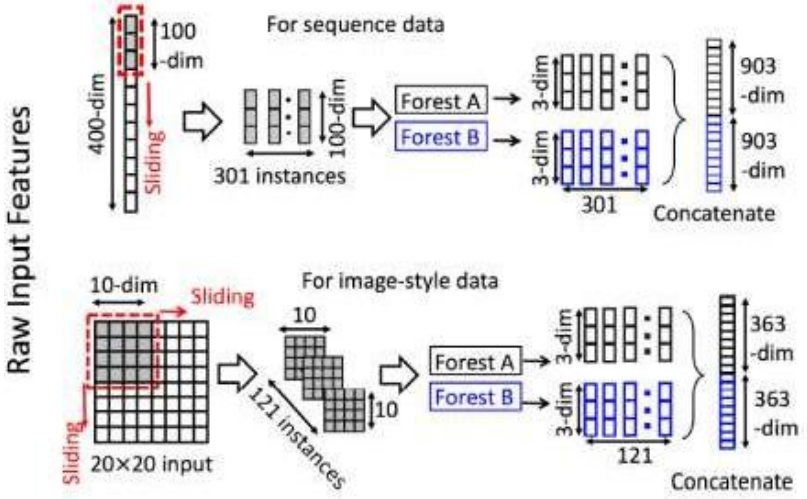

Figure.6. Multi-Grained scanning.

The Deep forest has shown a lot of promise, and its success can be attributed to the following factors:

- Fewerhyper-parameters

- Data-dependent tuning of model'scomplexity
- Less dependence onGPU

Experimental Analysis

Unsupervised learning with U-Net is a fully convolutional neural network composed of convolutional layers and depth concatenation, which is an essential and vital stage in the process of segmentation. Unsupervised learning with U-Net is an important and crucial phase in the task of segmentation. Low-level features such as edges and blobs may be found in the feature maps that are created at the beginning of the process and are particularly important for efficient segmentation. The picture size is reduced to 256 X 256 of the original size in this method. A total of 1000 photos were examined for training, testing, and validation of the aforementioned model, and the dataset was divided using the random sample approach into three groups with ratios of 0.75, 0.15, and 0.1.

All testing were carried out on a Dell OptiPlex 3060 system equipped with an Intel CORE i7 processor running at 3.20 GHz X 12 with 16GB of RAM and an AMD Radeon RX 550 series GPU, all of which were running on Ubuntu 18.04 LTS. In this technique, the Keras 2.3 framework is utilized in conjunction with the Tensorflow 1.13 back-end, and the programming language is Python 3.6. In order to make the model more resilient by comprehending all situations of photos that were collected in a variety of scenarios, no preprocessing techniques have been used to the images in this study. Matplotlib was used to create all of the graphs. Figure 7 shows the outcomes of the ground truth generating process using MATLAB 2019b, as well as a comparison of the findings. The model is applied on a variety of loss functions throughout the experimental evaluation phase. On the right are the segmentation results of several AZD pictures, and on the left are comparisons of the segmentation results using various optimization strategies in addition to the suggested mechanism.

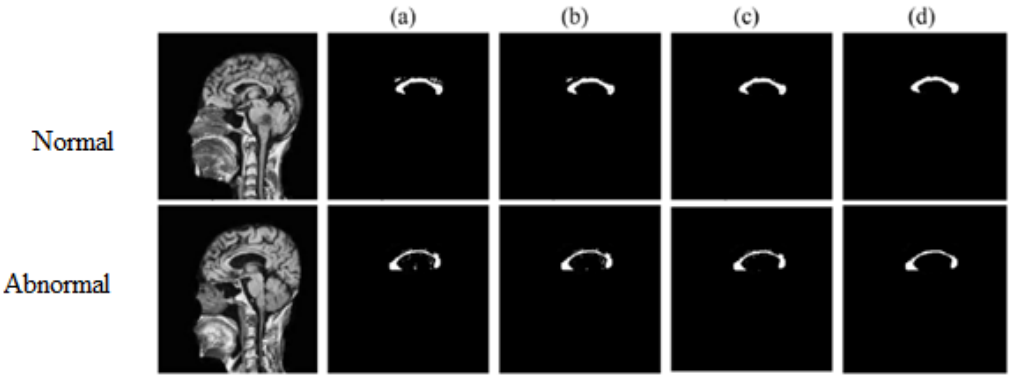

Figure 7: Comparison of Corpus Callosum Segmentation using the Proposed Framework (a) PSO (b) GA (c) CS (d) Proposed Framework

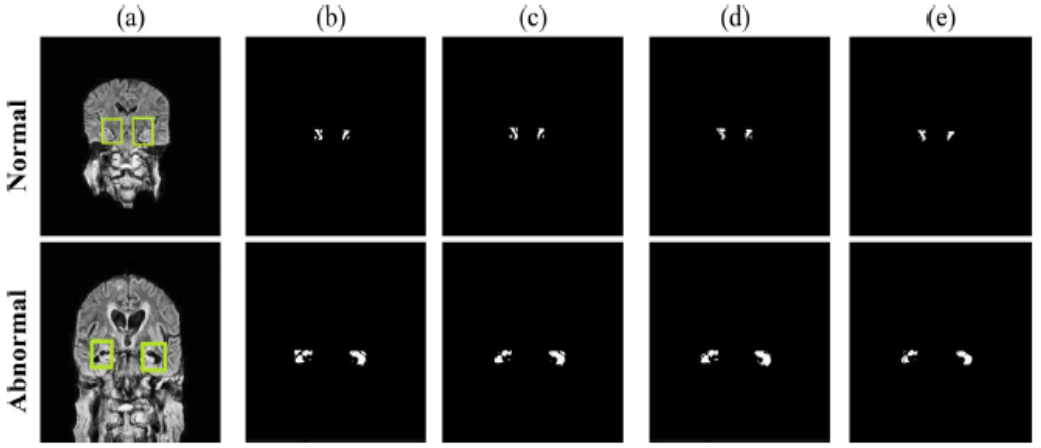

Figure 8: Comparison of Hippocampus Segmentation using the Proposed Framework (b) PSO (c) GA (d) CS (e) Proposed Framework

Alzheimer's disease has been predicted using the OASIS dataset [125]. The suggested model was trained using a variety of classification techniques on a total of 25,891 data (Bayes Net, naive Bayes, logistic, simple logistic, decision tree). There are a variety of assessment outcomes shown below in terms of properly categorised cases, true-positive rates, false-positive rates and other metrics. Precision, recall and F-score are also included. The suggested method is clearly better in terms of accuracy, recall, and F-score.

Several performance measures, including precision, recall, accuracy (AC), F1-score, Intersection over Union (IoU), and Dice Coefficient, were evaluated for quantitative analysis of the experimental data (DI). With the variables True Positive (TP), True Negative, False Negative, and False Positive, we can do this calculation (FN).

Table 1 Performance Evaluation

Evaluation Metrics /Algorithms	TP rate	FP rate	Precision	Recall	F-Measure	CCI%
Proposed Mechanism	0.934	0.465	0.90	0.897	0.89	90.5
Bayes Net	0.729	0.203	0.80	0.729	0.742	73.6
Logistic Regression	0.742	0.276	0.753	0.742	0.71	74.1
Decision Tree	0.672	0.374	0.77	0.672	0.67	65.66
RNN	0.886	0.466	0.83	0.886	0.84	88.56

Performance analysis of Proposed Segmentation Mechanism

In this section, the comparative analysis is carried out between proposed M-IWO with existing techniques such as Otsu Algorithm and Threshold algorithm in

terms of IoU and DI for two datasets. Table 2 and Figure 7 shows the validated analysis of proposed segmentationtechnique.

Table 2: Comparative Analysis of Proposed Segmentation Technique in terms of DI and IoU

Method	Dataset	IoU	DI
Otsu Algorithm	OASIS	0.6734	0.6845
Threshold		0.7645	0.7724
Proposed Modified IWO		0.8821	0.8929
Otsu Algorithm	ADNI	0.7167	0.7245
Threshold		0.7921	0.8097
Proposed Modified IWO		0.8883	0.8960

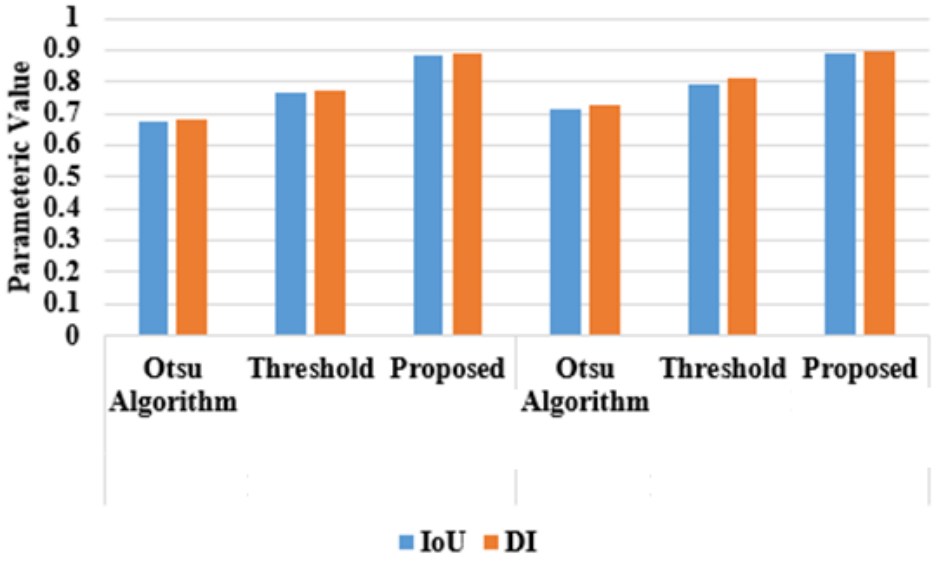

Figure 9: Graphical Representation of proposed segmentation model in terms of DI and IoU

In the ADNI dataset, the existing technique Otsu Algorithm achieved 0.6734IoU and 0.6845DI, Threshold algorithm achieved 0.7645IoU and 0.7724DI, where the proposed M-IWO algorithm achieved 0.8821IoU and 0.8929DI. In the analysis of OASIS dataset, the Otsu Algorithm achieved 0.7167IoU and 0.7245DI, Threshold algorithm achieved 0.7921IoU and 0.8097DI, where the proposed mean-shift algorithm achieved 0.8883IoU and 0.8960DI for the input images. The next section will describe the analysis of proposed classifier with existing techniques in terms of variousparameters.

Performance analysis of Proposed Classification Mechanism

In this section, the performance of proposed Deep Forest Classifier (DFC) is compared with existing Deep learning techniques such as Convolutional Neural Network (CNN) and Generative Adversarial Network (GAN) in terms of four parameters for two different datasets. Table 3 shows the experimental analysis of proposed classifier with existing techniques. Figure 8 shows the graphical representation of the DFC for OASIS dataset

Table 3: Comparative Analysis of Proposed DFC for two datasets in terms of variousparameter metrics

Method	Dataset	Precision	Recall	Accuracy	F1-measure
CNN	OASIS	0.9166	0.8654	0.8697	0.8890
GAN		0.9167	0.9164	0.9034	0. 9145
Proposed DFC		0.9668	0.9603	0.9603	0.9603
CNN	ADNI	0.8077	0.8200	0.7866	0.8114
GAN		0.9266	0.9416	0.9226	0.9312
Proposed DFC		0.9707	0.9636	0.9636	0.9644

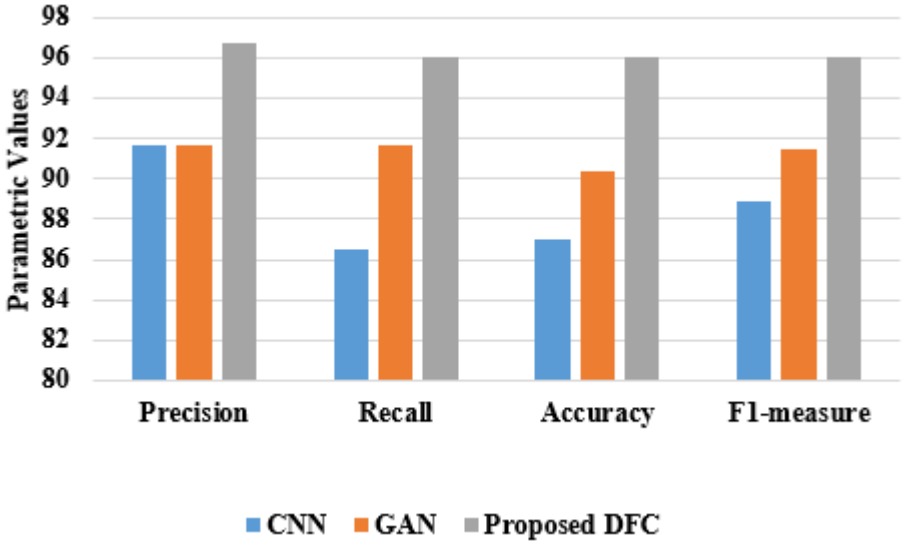

Figure 10: Graphical Representation of proposed DFC with existing techniques for OASIS Dataset

In the precision analysis of OASIS dataset, the CNN achieved 91.66%, GAN achieved 91.67% and proposed DFC achieved 96.68%, where CNN, GAN and DFC achieved 86.54% of recall, 91.64% of recall and 96.03% of recall values on the same dataset. The accuracy and F-measure of DFC is 96.03%, where the CNN achieved nearly 87% and GAN achieved nearly 91% of accuracy and F-measure. The reason for better performance of DFC is that CNN and GAN requires great

effort in hyper-parameter tuning, where DFC is much easier to train; even when it is applied to different data across different domains.

Conclusion

An optimization approach influenced by deep learning is presented in this research, and it is used to determine the appropriate threshold value, which assists in accurate picture segmentation and classification of MRIs of normal and MCD patients. This includes preprocessing using a 2D- Fuzzy Tsallis-entropy mechanism, based on which the region of interest such as the corpus callosum and Hippocampus is identified, as well as the application of an invasive weed optimization mechanism to perform multi-objective optimization in the context of determining the global optimum threshold value. This model is used to train and test the MRIs, as well as to categorize the NC MRIs with respect to MCD MRIs. Finally, ground truth information is created using the U-Net based CNN architecture. Results from the experiments show how well the suggested model assesses different factors, such as the best thresholding value for correct segmentation of MRIs linked to the corpus callosum and the Hippocampus, when used in conjunction with a computer. In addition, the results of this study might be used to the development of detrain mechanisms that could be used to minimize noise in MRIs when the images are segmented using appropriate thresholding techniques.

References

1. Burns and S. Iliffe, Alzheimer's disease, *BMJ* 338 (2009) b158
2. O. Valenzuela, X. Jiang, A. Carrillo and I. Rojas, Multi-objective genetic algorithms to find most relevant volumes of the brain related to Alzheimer's disease and mild cognitive impairment, *Int. J. NeuralSyst.* 28 (2018) 1850022.
3. M. Sado, A. Ninomiya, R. Shikimoto, B. Ikeda, T. Baba, K. Yoshimura and M. Mimura, The estimated cost of dementia in Japan, the most aged society in the world, *PLoS One* 13 (2018) e0206508
4. C. Fang, C. Li, M. Cabrerizo, A. Barreto, J.Andrian, N. Rishe, D. Loewenstein, R. Duara and M. Adjouadi, Gaussian discriminant analysis for optimal delineation of mild cognitive impairment in Alzheimer's disease, *Int. J. Neural Syst.* 28 (2018) 1850017.
5. J. P. Amezquita-Sanchez, N. Mammone, F. C. Morabito, S. Marino and H. Adeli, A novel methodology for automated differential diagnosis of mild cognitive impairment and the Alzheimer's disease using EEG signals, *J. Neurosci. Methods* 322 (2019) 88–95.
6. Y. Sun, Z. Dai, Y. Li, C. Sheng, H. Li, X. Wang, X. Chen, Y. He and Y. Han, Subjective cognitive decline: Mapping functional and structural brain changes — A combined resting-state functional and structural MR imaging study, *Radiology* 281 (2016) 185.
7. Y. Li, M. Mandal, S.N. Ahmed, Fully automated segmentation of corpus callosum in midsagittal brain MRIs, in: Proceedings of the Annual

International Conference of the IEEE Engineering in Medicine and Biology Society, EMBS, 2013, https://doi.org/10.1109/EMBC.2013.6610698.
8. R. Duara, D.A. Loewenstein, E. Potter, J. Appel, M.T. Greig, R. Urs, Q. Shen, A.
Raj, B. Small, W. Barker, E. Schofield, Y. Wu, H. Potter, Medial temporal lobe atrophy on MRI scans and the diagnosis of Alzheimer disease, Neurology (2008) http://dx.doi.org/10.1212/01.wnl.0000336925.79704.9f
9. Yue Li, Huiquan Wang, Nizam Ahmed, Mrinal Mandal, Automated corpus callosum segmentation in midsagittal brain MR images, ICTACT J. Image Video Process. (2017).
10. G.B. Frisoni, N.C. Fox, C.R. Jack, P. Scheltens, P.M. Thompson, The clinical use of structural MRI in Alzheimer disease, Nat. Rev. Neurol. (2010) http://dx.doi.org/10.1038/nrneurol.2009.215.
11. L. Younes, M. Albert, M.I. Miller, Inferring change point times of medial temporal lobe morphometric change in preclinical Alzheimer's disease, Neuro Image Clin. (2014) http://dx.doi.org/10.1016/j.nicl.2014.04.009
12. T. Kurban, P. Civicioglu, R. Kurban, E. Besdok, Comparison of evolutionary and swarm based computational techniques for multilevel color image thresholding, Appl. Soft Comput. J. (2014) http://dx.doi.org/10.1016/j.asoc.2014.05.037.
13. X.S. Yang, S. Deb, Cuckoo search via Levy flights, in: 2009 World Congr. Nat. Biol. Inspired Comput. NABIC 2009 - Proc., 2009, http://dx.doi.org/10.1109/NABIC.2009.5393690.
14. S. Suresh, S. Lal, An efficient cuckoo search algorithm based multilevel thresholding for segmentation of satellite images using different objective functions, Expert Syst. Appl. (2016) http://dx.doi.org/10.1016/j.eswa.2016.03.032.
15. Oliva D, Cuevas E, Pajares G, Zaldivar D, Perez-Cisneros M (2013) Multilevel thresholding segmentation based on harmony search optimization. J Appl Math 2013:1–24 230.
16. Oliva D, Cuevas E, Pajares G, Zaldivar D, Osuna V (2014) A multilevel thresholding algorithm using electromagnetism optimization. Neurocomputing 139:357–381
17. Mousavirad SJ, Ebrahimpour-Komleh H (2017) Multilevel image thresholding using entropy of histogram and recently developed population-based metaheuristic algorithms. EvolutIntell 10(1–2):45–75
18. Sarkar S, Das S, Paul S, Polley S, Burman R, Chaudhuri SS (2013) Multi-level image segmentation based on fuzzy-Tsallis entropy and diferential evolution. In: 2013 IEEE international conference on fuzzy systems (FUZZ). IEEE, pp 1–8
19. Bhandari AK, Kumar A, Singh GK (2015) Modifedartifcial bee colony based computationally efcient multilevel thresholding for satellite image segmentation using Kapur's, Otsu and Tsallis functions. Expert SystAppl 42(3):1573–1601
20. Zhang J, Li H, Tang Z, Lu Q, Zheng X, Zhou J (2014) An improved quantum-inspired genetic algorithm for image multilevel thresholding segmentation. Math ProblEng 2014:1–12
21. Mala C, Sridevi M (2016) Multilevel threshold selection for image segmentation using soft computing techniques. Soft Comput 20(5):1793–1810

22. Singh, V.K., Rashwan, H.A., Akram, F., Pandey, N., Sarker, M.M., Saleh, A., Abdulwahab, S., Maaroof, N., Torrents-Barrena, J., Romani, S., Puig, D. (2018) “Retinal Optic Disc Segmentation Using Conditional Generative Adversarial Network”. CCIA.
23. Gu, Zaiwang& Jiang, Shanshan& Lee, Jimmy &Xie, Jianyang& Cheng, Jun & Liu, Jiang. (2018)“Automatic Localization of Optic Disc using Modified U-Net”. 79-83. 10.1145/3232651.3232671.
24. Sun, Xu & Xu, Yanwu& Zhao, Wei & You, Tianyuan& Liu, Jiang. (2018) “Optic Disc Segmentation from Retinal Fundus Images via Deep Object Detection Networks”. Conference proceedings: Annual International Conference of the IEEE Engineering in Medicine and Biology Society. IEEE Engineering in Medicine and Biology Society. Conference. 10.1109/EMBC.2018.8513592
25. AnirbanMitra, Priya Shankar Banerjee, Sudipta Roy, Somasis Roy, Sanjit Kumar Setua, (2018) “The region of interest localization for glaucoma analysis from retinal fundus image using deep learning”, Computer Methods and Programs in Biomedicine, Volume 165, Pages 25-35, ISSN 0169-2607, https://doi.org/10.1016/j.cmpb.2018.08.003.